筑　波　大　学

博 士 （医 学） 学 位 論 文

Characterization of hypertrophic human iPS cell (hiPSC)-derived cardiomyocytes; Low-density plating is sufficient to induce hypertrophy and electrical remodeling in highly purified human iPS cell-derived cardiomyocytes

（肥大化ヒト人工多能性幹（iPS）細胞由来心筋細胞の性状解析;
高度に精製されたヒトiPS細胞由来心筋細胞において低密度培養は
肥大化および電気的リモデリングを誘導する）

２０１３

筑波大学大学院博士課程人間総合科学研究科

上杉 麻依

Contents

Abbreviations

18S rRNA	Eukaryotic 18S ribosomal RNA
ACTB	Actin, beta (β-actin)
ANKRD1	Ankyrin repeat domain 1 cardiac muscle (cardiac ankyrin repeat protein, CARP)
ATP2A2	ATPase, Ca^{2+} transporting, cardiac muscle, slow twitch 2 (sarcoplasmic reticulum calcium pump 2, SERCA2)
FPD	Field potential duration
FPDc	Corrected FPD
GAPDH	Glyceraldehyde-3-phosphate dehydrogenase
hESC	Human embryonic stem cell
hiPSC	Human induced pluripotent stem cell
iPSC	Induced pluripotent stem cell
ISI	Inter-spike interval
KCNE1	Potassium voltage-gated channel, Isk-related family, member 1
KCNE2	Potassium voltage-gated channel, Isk-related family, member 2
KCNH2	Potassium voltage-gated channel, subfamily H, member 2 (hERG)
KCNJ2	Potassium inwardly-rectifying channel, subfamily J, member 2
KCNQ1	Potassium voltage-gated channel, KQT-like subfamily, member 1
MYL2	Myosin, light chain 2, regulatory, cardiac, slow (MLC-2)
NPPA	Natriuretic peptide A (atrial natriuretic peptide, ANP)

Abstract

Introduction: Cardiac hypertrophy is a leading cause of many cardiovascular diseases, including heart failure, but its pathological mechanism is not fully understood. This study used highly purified human induced pluripotent stem cell (hiPSC)-derived cardiomyocytes to produce an *in vitro* hypertrophy model and characterize its gene expression and electrophysiological properties.

Methods: For 7 days we cultured hiPSC-derived cardiomyocytes plated at high (2800–4800 cells/mm^2) or low (500–1200 cells/mm^2) cell density and assessed their cell size with confocal and fluorescence microscopy, their electrophysiological and pharmacological responses with multi-electrode array systems, and their gene expression patterns by using DNA microarray technology and quantitative PCR. We used quantitative PCR and Western blotting to compare the expression of potassium-channel genes between the hiPSC-derived cardiomyocytes and human fetal and adult hearts.

Results: The hiPSC-derived cardiomyocytes showed spontaneous beating and similar pattern of α-actinin molecules regardless of plating density. However, cells plated at low density had the following characteristics compared with those at high density: 1) significant enlargement in size; 2) significant increase or decrease in expression of the cardiac hypertrophy-characteristic genes *NPPA*, *ATP2A2*, *ANKRD1* and *MYL2* in accordance with the progression of hypertrophy; 3) significant reduction in responses to the inhibitors of cardiac slow delayed-rectifier K^+ current (I_{Ks}), chromanol 293B and HMR1556, in a cell-density-dependent manner; and 4) significant reduction in the expression of the *KCNQ1* and *KCNJ2* genes coding the K^+ ion channels conducting each I_{Ks} and cardiac inward rectifier outward K^+ current (I_{K1}).

Discussion: The enlargement, hypertrophy-characteristic and potassium ion channels gene expression of hiPSC-derived cardiomyocytes suggest that low-density plating was sufficient to induce cardiac hypertrophy. This model may be useful in elucidating mechanisms underlying the onset and progress of cardiac hypertrophy, because these cells can be cultured for several weeks.

Introduction

Pathological cardiac hypertrophy is defined as thickening of the ventricular wall and septum with a net decrease in ventricular chamber size occurring in response to pressure or volume stress or specific gene mutations. It often accompanies cardiovascular diseases such as hypertension, myocardial infarction, heart valve stenosis, and heart failure (Frey et al., 2004; Heineke & Molkentin, 2006). Although cardiac hypertrophy is generally a compensatory process in its initial stages, this process leads to cardiac fibrosis, congestive heart failure, arrhythmia, and sudden death if it is sustained long-term (Drazner et al., 2004; Vakili et al., 2001). During cardiac hypertrophy, because adult cardiomyocytes are terminally differentiated and have lost their ability to proliferate, they grow in size without cell division to cope with the escalating demand for increased workload due to pressure or volume stress or pathological conditions (Bernardo et al., 2010).

Pathological cardiac hypertrophy models have been based on primary cultures of rat ventricular cardiomyocytes (Sadoshima et al., 1993; Shubeita et al., 1990). These cells increase in size in response to stimulation factors such as angiotensin II and endothelin 1 and demonstrate reactivation of the fetal cardiac gene program. An effective *in vitro* hypertrophy model using human cells would be useful for evaluating drugs for their causative or preventive effects on cardiac hypertrophy and for assessing cardiotoxic risk in patients with cardiac disorders. However, an opportunity of access to human cardiomyocytes for primary culture is limited and poorly amenable for this application. In contrast, human embryonic stem cell (hESC)- and human induced pluripotent stem cell (hiPSC)-derived cardiomyocytes recently became available and are likely *in vitro* tools for evaluating cardiotoxicity, including effects on cardiac hypertrophy, during drug development. When in a 3D cluster or a sheet, these cells show spontaneous and synchronized beating and respond to various ion-channel blockers, because they have many of the same ion channels that are expressed in native human cardiomyocytes (Ma et al., 2011; Yamazaki et al., 2012). In addition, hESC- and hiPSC-derived cardiomyocytes manifest features of hypertrophy under mechanical and chemical stress (Foldes et al., 2011; Tulloch et al., 2011). Compared with that in nonhuman-based models, the

hypertrophy induced in hESC- or hiPSC-derived cardiomyocytes likely will be more relevant to human cardiac hypertrophy.

Patients with cardiac hypertrophy are at high risk of clinical complications such as progressive heart failure, arrhythmia, and sudden cardiac death (Maron, 2002; Maron et al., 2003). Dogs with chronic complete atrioventricular block can develop ventricular hypertrophy, and the incidence of early-after depolarization (EAD) can increase and torsades de pointes can be observed after treatment with a class III antiarrhythmic compound (Volders et al., 1998); the cardiac inward rectifier outward K^+ current (I_{K1}) and the rapid and slow components of the delayed-rectifier K^+ current (I_{Kr} and I_{Ks}) are reduced owing to electrical remodeling (Volders et al., 1999). In cardiomyocytes, oligomeric association of the potassium voltage-gated channel, KQT-like subfamily, member 1 (*KCNQ1*; α-subunit) and potassium voltage-gated channel, Isk-related family, member 1 (*KCNE1*; β-subunit) yields a potassium channel that carries the I_{Ks} (Melman et al., 2002). I_{Ks} is important for the repolarization of cardiac action potential, and decreases in I_{Ks} due to mutations in the *KCNQ1* and *KCNE1* genes cause long-QT syndrome (Harmer et al., 2010; Roden et al., 1996). Dogs with chronic atrioventricular block have consistently shown significant concurrent reduction in the density of I_{Ks} and *KCNQ1* mRNA and protein levels (Ramakers et al., 2003; Stengl et al., 2006), although these two studies have reported a decrease (Ramakers et al., 2003), or no change (Stengl et al., 2006), in *KCNE1* mRNA and protein levels with decreased I_{Ks}. Although right ventricular human cardiac cells with severe histological and functional abnormalities have demonstrated decreased I_{Ks} (Li et al., 2004), the expression levels of the *KCNQ1* and *KCNE1* genes during cardiac hypertrophy have not yet been clarified. Hypertrophy models comprised of hiPSC-derived cardiomyocytes likely will be useful for exploring changes in these currents.

In this study, we used hiPSC-derived cardiomyocytes to produce an *in vitro* human hypertrophy model. hiPSC-derived cardiomyocytes are non-dividing, beat spontaneously, express many cardiomyocyte-related genes, and are nearly pure cultures of cardiomyocytes (Anson et al., 2011; Kattman et al., 2011). These characteristics differ from those of primary cultures of human cardiomyocytes, which contain fibroblasts (Ancey et al., 2003), and human fetal cardiomyocytes,

which proliferate (Erokhina et al., 2005). In addition, the multi-electrode array system has been used successfully to pharmacologically evaluate I_{Ks} blockers in hESC-derived and hiPSC-derived cardiomyocytes (Egashira et al., 2012; Yamazaki et al., 2012), further indicating the advantages of these cells over primary cardiomyocytes isolated from dogs, rabbits, and humans, which have low sensitivity to I_{Ks} blockers (Jost et al., 2005). Here, we used gene expression analysis and electrophysiological measurement by the multi-electrode array system to confirm the cell hypertrophy and the reduction of I_{Ks} in our hiPSC-derived cardiomyocytes. We found that these cells showed a hypertrophy-like phenotype under low-density culture conditions and decrease sensitivity to I_{Ks} blockers in electrophysiological assay.

Methods

1. Cell and reagents

As pre-culture, hiPSC-derived cardiomyocytes (iCell Cardiomyocytes, Cellular Dynamics International, Madison, WI, USA) were plated according to the manufacturer's protocol on gelatin (Sigma-Aldrich, St. Louis, MO, USA)-coated 6-well plates in iCell Cardiomyocyte Plating Medium (Cellular Dynamics International) at a density of 4.5×10^6 to 6.0×10^6 cells/well (that is, 4688–-6250 cells/mm^2) and incubated at 37 °C in 5% CO_2 for 2 to 21 days. Every 2 days after plating, half of the volume of the medium was removed and replaced with iCell Cardiomyocytes Maintenance Medium (Cellular Dynamics International).

For cell imaging, hiPSC-derived cardiomyocytes were isolated by treatment with 0.25% trypsin–EDTA (Sigma-Aldrich) after 2 days of pre-culture and re-plated on gelatin-coated 96-well glass-bottom plates in iCell Cardiomyocytes Maintenance Medium at a density of 90,000 cells/well (high density, 2813 cells/mm^2) or 22,500 cells/well (low density, 703 cells/mm^2) and incubated at 37 °C in 5% CO_2. Every 2 days after plating, half of the volume of the medium was removed and replaced with iCell Cardiomyocytes Maintenance Medium. After the cells had been cultured for 7 days, they were fixed with 4% paraformaldehyde (Wako Pure Chemical Industries, Osaka, Japan) and washed in phosphate-buffered saline (PBS; Wako Pure Chemical Industries) for immunohistochemistry. Some cultures were left unfixed for confocal microscopy.

For the extracellular field-potential recordings, hiPSC-derived cardiomyocytes were isolated by using 0.25% trypsin-EDTA after 6 to 21 days of pre-culture, and 2 μL of cell suspension was plated on a small area (that is, approximately 2 mm in diameter) coated with fibronectin (Life Technologies, Carlsbad, CA, USA) covering the area of electrodes (1.05 mm×1.05 mm) on MED64 probes (MED-P515A, Alpha MED Sciences, Osaka, Japan) at a density of 30,000 cells/probe (very high density, 9554 cells/mm^2), 15,000 cells/probe (high density, 4777 cells/mm^2), 7500 cells/probe (medium density, 2389 cells/mm^2) or 3750 cells/probe (low density, 1194 cells/mm^2). Cell densities in cells/mm^2 were calculated, assuming that the cells were plated in a circular area 2 mm in diameter.

Beginning 5 to 7 days after being plated on the electrodes, sheets of synchronously beating cells were subjected to field-potential recordings.

For total RNA extraction, hiPSC-derived cardiomyocytes (without pre-culture) were plated on gelatin-coated 6-well plates in iCell Cardiomyocyte Plating Medium at a density of 2.7×10^6 cells/well (high density, 2813 cells/mm^2) or 0.5×10^6 cells/well (low density, 521 cells/mm^2) and incubated at 37 °C in 5% CO_2. Every 2 days after the plating, half of the volume of the medium was removed and replaced with iCell Cardiomyocytes Maintenance Medium. At 7 days after plating, cells were washed with PBS and lysed with RLT buffer (RNeasy Mini Kit, Qiagen, Hilden, Germany) containing 1% 2-mercaptoethanol (Nacalai Tesque, Kyoto, Japan).

For protein extraction, hiPSC-derived cardiomyocytes (without pre-culture) were plated on gelatin-coated 24-well plates in iCell Cardiomyocyte Plating Medium at a density of 5.3×10^5 cells/well (high density, 2819 cells/mm^2) or 98,000 cells/well (low density, 521 cells/mm^2) and incubated at 37 °C in 5% CO_2. Every 2 days after plating, half of the volume of the medium was removed and replaced with iCell Cardiomyocytes Maintenance Medium. Seven days after plating, cells were washed with PBS, trypsinized, and counted under a microscope. After the cell count, cells were lysed with RIPA buffer (Thermo Fisher Scientific, Waltham, MA, USA) containing protease inhibitors (Complete, Roche Diagnostics, Mannheim, Germany).

2 Confocal fluorescence microscopy

hiPSC-derived cardiomyocytes were stained with CellMask Plasma Membrane Deep Red (dilution, 1:1000; Life Technologies) for 30 min at 37 °C in 5% CO_2. Confocal images were acquired by using a confocal fluorescence microscope (LSM 510 META, ZEISS, Oberkochen, Germany) with a 63× objective. The total area of cells was determined by using the area measurement tool of ImageJ software (version 1.46, freeware program of National Institutes of Health, USA; http://rsbweb.nih.gov/ij/). Statistical significance was calculated by using Welch's *t*-test (Prism 6, GraphPad Software, La Jolla, CA, USA).

3 Immunocytochemistry

hiPSC-derived cardiomyocytes after fixed in 4% paraformaldehyde permeabilized by being treated for 30 min with Tris-buffered saline (TBS; Bio-Rad Laboratories, Hercules, CA, USA) containing 0.1% Triton X-100 (Wako Pure Chemical Industries), and blocked with 4% Block Ace (DS Pharma Biomedical, Osaka, Japan) for 60 min. The hiPSC-derived cardiomyocytes were stained with anti-α-actinin antibody (dilution, 1:1000; Sigma-Aldrich) overnight at room temperature, washed three times with TBS containing 0.05% Tween 20 (TBS-T; Bio-Rad Laboratories), and then stained with Alexa Fluor 488 Donkey Anti-Mouse IgG (H+L) (1:500; Life Technologies), CellMask Deep Red (1:5000; Life Technologies), and Hoechst 33342 (1:100; Sigma-Aldrich) for 30 min. After being stained, hiPSC-derived cardiomyocytes were washed three times with TBS-T and viewed under a fluorescence microscope (IX81; Olympus, Tokyo, Japan) with a 20× objective.

4. Extracellular field-potential recordings

The extracellular field potential of sheet cells was recorded by using the MED64 System (Alpha MED Sciences) and its accompanying software (Mobius QT, Alpha MED Sciences) according to previous report (Yamazaki et al., 2012). Briefly, the field potential duration (FPD) regarded as a QT-like interval in electrocardiogram was defined as the interval from the initial sharp deflection to the later peak of positive or negative deflection in waveforms. Output signals were digitized at 20 kHz. In addition, beat frequencies and inter-spike intervals (ISIs) were recorded. Thirty minutes before the start of field potential measurement, the culture medium was replaced with fresh iCell Cardiomyocytes Maintenance Medium pre-warmed to 37 °C. After equilibration, the preparations were placed on a hot plate and kept at 37 °C; they were covered with a lid through which aeration of 95% O_2, 5% CO_2 gas was provided. Before the addition of vehicle or a compound to the medium, waveforms and the regularity of the beating rates and FPDs were checked for more than 30 min. Compound solutions were added cumulatively to the medium at one-thousandth volume (2 μL). After the addition of compound, the medium was mixed by careful pipetting.

Compounds tested were the I_{Ks} blockers Chromanol 293B (1, 3, 10 and 30 μM; Sigma-Aldrich) and HMR1556 (0.1, 0.3, 1 and 3 μM; synthesized by Eisai Co., Ltd.) and the I_{Kr} blocker E4031 (0.3, 1, 3, 10 and 30 nM; Wako Pure Chemical Industries), which were dissolved in dimethyl sulfoxide (DMSO; Wako Pure Chemical Industries). Baseline for each compound was measured by addition of 2 μL DMSO. In previous report, we confirmed that the cumulative sixth addition of 2 μL DMSO did not affect the FPD (Yamazaki et al., 2012). The FPD for the baseline and each concentration of a compound was measured for 10 min, near the end of which time we extracted 30 FPDs and ISIs for analysis. A corrected FPD (FPDc) was calculated according to Fridericia's formula ($FPDc = FPD/ISI^{1/3}$), and the 30 FPDc values were averaged. The prolongations of FPDc were almost the same between shortest (6 days) and longest (21 days) pre-culture for the response to HMR1556 and E4031 in high-density-cultured cells in this study. The % FPDcs to control in 6 or 21 days-pre-cultured cells were 136.09% (n = 6) and 134.12% (n = 2) with HMR1556 (3 μM), and 121.91% (n = 2) and 134.72% (n = 2) with E4031 (30 nM), respectively. Therefore, all the data for different pre-culture conditions were pooled for analysis. Statistical significance was calculated by using *t*-tests for unpaired unequal variance (Welch's *t*-test) in Prism 6 (GraphPad Software) to compare FPD, ISI and FPDc values between different density cells, and the Jonckheere-Terpstra trend test (Jonckheere, 1954; Terpstra, 1952) in the R 2.15.2 using SAGx package (http://www.R-project.org/; http://www.bioconductor.org/packages/release/bioc/html/SAGx.html) to show cell-density-dependent effects on FPDc.

5. RNA extraction

Total RNA was prepared from hiPSC-derived cardiomyocytes by using RNeasy mini spin columns (Qiagen) according to the manufacturer's protocol. The yield and quality of each isolated total RNA sample was determined by using a NanoDrop 1000 spectrophotometer (Thermo Fisher Scientific) and RNA Nano LabChips analyzed on a 2100 Bioanalyzer (Agilent Technologies, Santa Clara, CA, USA). NanoDrop spectrophotometers measure absorbency at wavelengths of 280 nm and 260 nm; ratios of these absorbencies (that is, A_{260}:A_{280}) are used to assess sample purity. An

A_{260}:A_{280} ratio of approximately 2.0 is considered pure for RNA samples. The 2100 Bioanalyzer obtains the RNA Integrity Number (RIN) from the pattern of total RNA electrophoresed as a metric for RNA degradation (Schroeder et al., 2006). A RIN of 9.5–10.0 is considered pure for total RNA from the hiPSC-derived cardiomyocytes.

6. Total RNA from human fetal and adult hearts

Human adult-heart total RNA were obtained from 3 vendors: 1) Human Heart Total RNA (lot# 1112059A, Clontech, Mountain View, CA, USA); 2) Total RNA, Human Heart (lot# 0006097996, Agilent Technologies); and 3) Total RNA—Human Adult Normal Tissue, Heart (lot# B604038, BioChain, Newark, CA, USA). In addition, human fetal-heart total RNA were obtained from 3 vendors: 1) Human Fetal Heart Total RNA (lot# 1005013, Clontech); 2) Total RNA, Human Fetal Heart (lot# 0006111328, Agilent Technologies); and 3) Total RNA—Human Fetal Normal Tissue, Heart (lot# B512117, BioChain).

7. Microarray analysis

100 ng total RNA was converted to cyanine-3 (Cy3)-labeled complementary RNA (cRNA) by using a Low Input Quick Amp Labeling Kit, One-Color (Agilent Technologies) according to the manufacturer's instructions for single-color 8×60K gene expression arrays. Cy3-labeled cRNAs were purified by using an RNeasy Mini purification kit (Qiagen) and hybridized to the SurePrint G3 Human Gene Expression 8×60K Microarray (Agilent Technologies) at 65 °C for 17 h by using a Gene Expression Hybridization Kit (Agilent Technologies) according to the manufacturer's instructions. Arrays were washed with a Gene Expression Wash Pack (Agilent Technologies) and scanned on a DNA Microarray Scanner (Agilent Technologies) according to the manufacturer's instructions. Quantification of scanned images was accomplished by using Feature Extraction software (version 11, Agilent Technologies). The resulting files were imported and analyzed with GeneSpring (version 12.5, Agilent Technologies). Raw data were normalized by using a quantile method. The *P*-values for all statistical tests were estimated by using Welch's *t*-test, followed by

adjustment for multiple comparisons by using the false-discovery rate (FDR) approach (Benjamini-Hochberg procedure). A gene was considered to be differentially expressed when its absolute fold change relative to the control value was ≥1.5 with an FDR *P*-value of ≤0.05. Pathway analysis was conducted by using Ingenuity Pathway Analysis (Ingenuity Systems, Redwood City, CA, USA).

8. Quantitative real-time RT-PCR analysis

The cDNA synthesis was run in 10-μL volumes containing 500 ng total RNA by using a High Capacity cDNA Reverse Transcription Kit with RNase Inhibitor (Life Technologies) according to the manufacturer's instructions. Quantitative PCR analysis of 7.2 ng cDNA (total RNA equivalent) per well in duplicate (n = 3 biological replicates) by using TaqMan Fast Advanced Master Mix (Life Technologies) on a ViiA7 Real-time PCR System (Life Technologies) was performed. TaqMan Gene Expression Assays were purchased from Life Technologies; *KCNQ1*: Hs00923522_m1; *KCNE1*: Hs00897540_s1; *KCNE2*: Hs00270822_s1; *KCNH2*: Hs00165120_m1; *KCNJ2*: Hs00265315_m1; *NPPA*: Hs00383231_m1; *ATP2A2*: Hs00155939_m1; *ANKRD1*: Hs00173317_m1; *MYL2*: Hs00166405_m1; *GAPDH* (glyceraldehyde-3-phosphate dehydrogenase): Hs99999905_m1; 18S rRNA (Eukaryotic 18S ribosomal RNA): Hs99999901_s1 and *ACTB* (actin, beta): Hs99999903_m1. Cycle threshold (Ct) values were determined by using ViiA7 software version 1.1 (Life Technologies). A 6-point standard curve was used to determine PCR efficiency and relative quantitation. Relative gene expression normalized against the expression level of 18S rRNA was calculated by using Excel 2010 (Microsoft, Redmond, WA, USA). Statistical significance was calculated by using Welch's *t*-test in Prism 6.

9. Protein extraction and Western blotting

Whole-cell lysates were prepared from hiPSC-derived cardiomyocytes by using RIPA buffer (Thermo Fisher Scientific) containing protease inhibitors (Complete, Roche Diagnostics), in accordance with each manufacturer's protocol. The protein concentration of each lysate was

determined by using a Pierce BCA Protein Assay Kit (Thermo Fisher Scientific) and a SpectraMax 190 (Molecular Devices, Sunnyvale, CA, USA) with SoftMax Pro software (version 5.2, 4-parameter mode, Molecular Devices). Statistical significance was analyzed by using Welch's *t*-test (Prism 6).

The volume of lysate containing 10 μg of protein samples was denatured with Laemmli Sample Buffer (Bio-Rad Laboratories) containing 2.5% 2-mercaptoethanol, fractionated by SDS-PAGE on 5%–20% polyacrylamide gels (e-PAGEL, ATTO, Tokyo, Japan) with a Spectra Multicolor High Range Protein Ladder (Thermo Fisher Scientific), and then transferred electrophoretically to polyvinylidene difluoride membranes, with Tris–Glycine buffer (Bio-Rad Laboratories) containing 20% methanol (Wako Pure Chemical Industries) as the transfer buffer. Membranes were blocked in TBS-T containing 5% skim milk (Wako Pure Chemical Industries) and incubated overnight at 4 °C with primary antibodies (anti-KCNQ1 antibody, 1:200, Santa Cruz Biotechnology, Dallas, TX, USA; anti-KCNH2, 1:400, Alomone Labs, Jerusalem, Israel) in TBS-T containing 1% skim milk. After being washed, membranes were incubated with horseradish peroxidase–conjugated anti-rabbit IgG secondary antibody (1:5000, Cell Signaling Technology, Danvers, MA, USA). Antibody was detected by using Amersham ECL Prime Western Blotting Detection Reagent (GE Healthcare, Buckinghamshire, UK) on a luminescent image analyzer (LAS-4000 IR, FUJIFILM, Tokyo, Japan/GE Healthcare). Scanned images were quantified and expressed in arbitrary unit by using MultiGauge software (version 3.0, FUJIFILM). Statistical significance was calculated by using Welch's *t*-test in Prism 6.

Results

1. Low-density cell plating leads to enlargement of hiPSC-derived cardiomyocytes

To evaluate the morphology of hiPSC-derived cardiomyocytes plated at high (90,000 cells/well) and low (22,500 cells/well) densities and cultured on 96-well plates for 7 days, images of living cells were obtained by confocal fluorescence microscopy. In the high-density cultures the cells were round or polygonal, and most had a diameter of less than 50 μm. In contrast, the picture of microscopy showed much larger cells in the low-density cultures than those in high-density cultures; some cells at low density were longer than 100 μm in longitudinal length (Fig. 1A). Cell heights were less than 10 μm and did not differ between low- and high-density cultures (Fig. 1A). Cell area in low-density cultures was significantly increased compared with that of cells at high density (cell area in high- and low-density cultures, 711.88 and 1654.44 μm^2; $P \leq 0.001$, Fig. 1B). hiPSC-derived cardiomyocytes plated at low density stained positively with α-actinin, with staining distributed evenly throughout the cells and similar to that of cells plated at high density (Fig. 1C). The concentration of protein was measured in hiPSC-derived cardiomyocytes plated at high (5.3×10^5 cells/well) and low (98,000 cells/well) densities and cultured on 24-well plates for 7 days. Protein amount per single cell was significantly greater in cells at low than at high density (protein amount in high- and low-density cultures, 0.42 and 0.65 ng/cell, $P \leq 0.05$, Fig. 1D).

2. Gene expression analysis reveals similarities between low-density cultured hiPSC-derived cardiomyocytes and cardiac hypertrophy

We performed DNA microarray analysis to examine differences in gene expression levels between cardiomyocytes grown under high- and low-density culture conditions, respectively. Pathway analysis was conducted by using the Tox Functions program of Ingenuity Pathway Analysis software and the list of gene probes in low-density cultured cells that showed a fold change (FC) of ≥1.5 and an FDR *P*-value of ≤0.05 compared with expression levels in high-density cultured cells. The list included 2370 and 2072 probes for genes with increased and decreased

expression, respectively (data not shown). Table 1 shows the top 10 toxicological functions that showed significant relationship with the gene list. All of the top 4 toxicological functions—hypertrophy of heart chamber, hypertrophy of heart, hypertrophy of left ventricle and ventricular hypertrophy—were members of the cardiac hypertrophy category. Figure 2A shows the expression of 3 housekeeping genes, *GAPDH* (glyceraldehyde-3-phosphate dehydrogenase), *ACTB* (actin, beta), and 18S rRNA (Eukaryotic 18S ribosomal RNA) in high- and low-density-cultured hiPSC-derived cardiomyocytes, fetal and adult heart. The expression level of *GAPDH* gene was significantly greater in high- and low-density hiPSC-derived cardiomyocytes than in human fetal and adult hearts (expression value of *GAPDH* in high- and low-density cells, fetal and adult hearts, 1917.59, 1551.12, 856.45 and 738.82, respectively) and *ACTB* gene was significantly greater in low-density than in high-density hiPSC-derived cardiomyocytes and human fetal heart (*ACTB* in high- and low-density cells and fetal and adult hearts, 1294.97, 2627.65, 1350.34 and 1622.15, respectively). In contrast, 18S rRNA was not altered among all samples. We selected 18S rRNA as the normalizer for later qPCR analysis because it was expressed invariably in all types of the RNA samples used in this study. The expression of genes associated with cardiac hypertrophy, including *NPPA* (natriuretic peptide A/atrial natriuretic peptide, ANP), *ATP2A2* (ATPase, Ca^{2+} transporting, cardiac muscle, slow twitch 2/sarcoplasmic reticulum calcium pump 2, SERCA2), *ANKRD1* (ankyrin repeat domain 1, cardiac muscle/cardiac ankyrin repeat protein, CARP), and *MYL2* (myosin, light chain 2, regulatory, cardiac, slow/MLC-2) (Aihara et al. 2000; Ju et al. 1996; Sadoshima et al. 1993; Shubeita et al. 1990) was shown in Figure 2B. *NPPA*, *ANKRD1* and *MYL2* expression was greater, and *ATP2A2* expression less, in the low-density cultured hiPSC-derived cardiomyocytes than in the high-density cultured cells (relative expression values: *NPPA*, 0.26 and 1.59, respectively, $P \leq 0.01$; *ATP2A2*, 1.39 and 0.94, respectively, $P \leq 0.05$; *ANKRD1*, 1.00 and 1.56, respectively, $P \leq 0.01$; *MYL2*, 0.72 and 1.22, respectively, $P \leq 0.01$). The directions of the expression-level changes were consistent with progression to pathologic hypertrophy.

3. Low-density cultured hiPSC-derived cardiomyocytes have decreased sensitivity to I_{Ks}

blockers

We evaluated the effects of I_{Ks} and I_{Kr} blockers on FPDc in hiPSC-derived cardiomyocytes plated at densities of 30,000 (very high density), 15,000 (high density), 7500 (medium density), and 3750 (low density) cells/probe. The success rate of field-potential recording decreased as cell density was reduced, and fewer data were obtained from cells plated at low density. Fig. 3 shows the basal FPD, ISI and FPDc at different cell densities. FPD, ISI and FPDc at low density were significantly greater than those at very-high-density (FPD, ISI and FPDc in very high- and low-density cultures, 270.04 and 306.17 msec, $P \leq 0.001$; 773.59 and 876.71 msec, $P \leq 0.05$; and 295.05 and 320.43 msec, $P \leq 0.01$, respectively). FPDc was prolonged by the I_{Ks} blockers chromanol 293B and HMR1556 and by the I_{Kr} blocker E4031 in a concentration-dependent manner above 3 μM, 0.3 μM, and 3 nM, respectively, at all cell densities (Fig. 4A). In addition, the slopes of FPDc prolongation decreased in a cell density-dependent manner with chromanol 293B and HMR1556. The prolongation of FPDc with chromanol 293B was 126.65%, 124.21%, and 118.92% at a concentration of 30 μM in cultures of very high, high, and medium cell densities, respectively, and had a significant trend between decrease of cell density and decrease of FPDc prolongation ($P \leq 0.05$). With HMR1556, the prolongation at 1 μM was 125.13%, 123.32%, 121.13% and 115.01%, and at 3 μM was 132.57%, 124.94%, 122.94% and 113.99% in cultures of very high, high, medium, and low cell densities, respectively, and had a significant trend between decrease of cell density and decrease of FPDc prolongation ($P \leq 0.05$ and $P \leq 0.001$, respectively). In contrast to the responses to I_{Ks} blockers, there was no significant difference in the increases in FPDcs at very high, high, medium, and low cell densities with E4031 at 30 nM (FPDc prolongation was 119.10%, 115.72%, 110.87% and 133.09%, respectively), but low-density cells showed greater prolongation of FPDcs with statistical significance ($P \leq 0.05$ or $P \leq 0.01$) compared with other densities. Two in 5 preparations at low density showed waveforms of early after depolarization (Fig. 4B), and were not included in the analysis of FPDc.

4. Expression of genes associated with potassium channels, including I_{Ks} channel subunits, in

hypertrophic phenotypes of low-density cultured hiPSC-derived cardiomyocytes

To examine changes in potassium channels of the low-density cultured hiPSC-derived cardiomyocytes, we used quantitative PCR analysis to measure the expression levels of the *KCNQ1*, *KCNE1*, *KCNE2*, *KCNH2* (potassium voltage-gated channel, subfamily H, member 2/hERG), and *KCNJ2* (potassium inwardly rectifying channel, subfamily J, member 2) genes. The expression levels of these genes in the hiPSC-derived cardiomyocytes at 2.7×10^6 cells/well (high density) or 0.5×10^6 cells/well (low density) were compared with those of human fetal and adult hearts. Expression of *KCNQ1* was decreased (relative expression value of *KCNQ1* in high- and low-density cells, 1.66 and 1.14, respectively, $P \leq 0.05$), but that of *KCNE1* was upregulated (*KCNE1* in high- and low-density cells, 0.88 and 2.40, respectively, $P \leq 0.001$) in hiPSC-derived cardiomyocytes plated at low density compared with those at high density (Fig. 5A). In addition, expression of *KCNJ2*, which conducts I_{K1} current, was downregulated (*KCNJ2* in high- and low-density cells, 0.41 and 0.17, respectively, $P \leq 0.001$) in low-density cells compared with those in high-density cells (Fig. 5A). Expression of *KCNQ1*, *KCNH2* and *KCNE2* was significantly greater in high- and low-density hiPSC-derived cardiomyocytes than in human fetal and adult hearts (*KCNQ1* in high- and low-density cells, fetal and adult hearts, 1.66, 1.14, 0.90 and 0.74, respectively; *KCNH2*, 1.66, 2.02, 0.56 and 0.63; *KCNE2*, 1.68, 1.29, 0.50 and 0.24). Expression of *KCNE1* in low-density cells was greater than in human adult heart (low-density cells and adult heart, 2.40 and 1.34, $P \leq 0.05$) but was equivalent between low-density cells and human fetal heart (Fig. 5A). The protein level of KCNQ1 was lower in low-density than in high-density cells (intensity of KCNQ1 protein band in high- and low-density cells, 8212822.29 and 4775372.12, respectively, $P \leq 0.05$) (Fig. 5B and 5C). The protein level of KCNH2 was equivalent between high- and low-density cells (Fig. 5B and 5C).

Discussion

We found here that hiPSC-derived cardiomyocytes showed a hypertrophy-like phenotype only after the cells were exposed to low-density culture conditions and that the expression levels of cardiac hypertrophy-related genes in low-density hiPSC-derived cardiomyocytes were altered in accordance with disease progression. Cardiac hypertrophy is a leading cause of many cardiovascular diseases and a key cause of heart failure (Drazner et al., 2004; Frey et al., 2004; Heineke & Molkentin, 2006; Vakili et al., 2001). Because hypertrophic hearts may be highly sensitive to the toxic effects of drugs, evaluating candidate new compounds in this model of cardiac hypertrophy may prove valuable.

One of the characteristic features of cardiac hypertrophy is the enlargement of cardiomyocytes; an approximate 1.5 times the size of cardiomyocytes has been reported in *in vitro* and *in vivo* studies of dogs, rats, and rabbits (Flores-Munoz et al., 2012; Hao et al., 2007; Volders et al., 1998; Zou et al., 2006). In our model, cells in low-density cultures were 2.4 times larger on average than were those in high-density cultures, according to the average size of high-density cultures without factoring in changes in cell height. Some cells in low-density cultures were more than 5 times larger than were those plated at high density. This marked enlargement of hiPSC-derived cardiomyocytes may reflect the large extracellular space in low-density cell plating compared with the limited space for expansion in *in vivo* studies. Another possible explanation for the marked cell enlargement is the small size of the cardiomyocytes (including hiPSC-derived cardiomyocytes) at early developmental stages, as stem-cell-derived cardiomyocytes do not as yet developed as adult cardiomyocytes (Khan et al., 2013) and can grow greatly in size during postnatal development to adult size in the absence of proliferation. In hypertrophic models using neonatal rat cardiomyocytes (Watkins et al., 2011) or human stem-cell-derived cardiomyocytes (Foldes et al., 2011), a doubling in cell size over 2 days was observed. The greater enlargement of the hiPSC-derived cardiomyocytes here than in previous studies may be related to the duration of culture (7 days) at low density. Increased protein synthesis has been reported as another feature of

hypertrophy (Bernardo et al., 2010) and supports that of the low-density cultured hiPSC-derived cardiomyocytes. Even though they are greatly enlarged, the function of the cells seems to be normal, because the low-density cultured hiPSC-derived cardiomyocytes beat spontaneously (data not shown) and because staining for sarcomeric cardiac actinin (α-actinin) was distributed similarly throughout the cells regardless of plating density.

Pathological cardiac hypertrophy is due to responses to a stimulation factor, such as angiotensin II or endothelin 1, and shows a phenotype of hypertrophic growth characterized by increased cell size and expression of fetal cardiac genes (e.g., *NPPA*, *ATP2A2*, *ANKRD1* and *MYL2*) to compensate for reduced cardiac function (Aihara et al., 2000; Ju et al., 1996; Sadoshima et al., 1993; Shubeita et al., 1990). The expression levels of *NPPA*, *ATP2A2*, *ANKRD1* and *MYL2* in the low-density cultured hiPSC-derived cardiomyocytes were similar to those in previous reports (Aihara et al., 2000; Ju et al., 1996; Sadoshima et al., 1993; Shubeita et al., 1990), showing progression toward pathology in these cells. Furthermore, our pathway analysis using Ingenuity Pathway Analysis software supported our claim that the low-density cultured hiPSC-derived cardiomyocytes had a hypertrophic phenotype. In addition, reduction of *KCNQ1* gene expression was in line with a report that I_{Ks} and *KCNQ1* gene expression were reduced in a cardiac hypertrophy model (Ramakers et al., 2003; Stengl et al., 2006; Volders et al., 1999). We feel that these combined results indicate that the enlarged hiPSC-derived cardiomyocytes after low-density culture are effective models of hypertrophied cardiac cells, even though specific manipulations, such as pharmacological treatment to induce hypertrophy, were not used.

Several possibilities regarding the mechanisms of induction of hypertrophy in the cardiomyocytes here need to be considered. First, the extracellular coating materials may have caused the observed cardiac hypertrophy, given that fibronectin (but not gelatin) induces cardiac hypertrophy in *in vitro* rat models (Chen et al., 2004; Ogawa et al., 2000). We were able to observe enlargement of cells using either gelatin or fibronectin, suggesting that the coating material may not be the key cause of hypertrophy. In addition, if the coating material had been the sole cause of the change in gene expression, then similar changes likely would have occurred in low- and

high-density cultures. Second, the attachment of the cells to the plate surface might have initiated signals to promote hypertrophy. If this were the case, the signals would have increased in intensity as the cells plated at low density and enlarged until they contacted other cells. However, these signals likely do not occur in high-density cultures, because the cells were densely seeded and contacted other cells from the onset. Third, some component(s) of the culture medium might have contributed to the induction of hypertrophy. The exact factors that induce hypertrophy in cardiomyocytes have not yet been clarified, but it will be interesting to explore the mechanism(s) to gain insights into hypertrophy.

Electrical remodeling in hypertrophied cardiomyocytes is well characterized, and changes in expression levels of various ion channels underlie this phenomenon. In dog cardiac hypertrophy, prolongation of action potential duration and downregulation of sarcolemmal K+ currents, including I_{Ks} (Volders et al., 1998; 1999), has been reported. Here, we did not measure the level of I_{Ks} by using patch-clamp experiments, but the increase in FPD/FPDc, the decreased sensitivity to I_{Ks} blockers and the reduction of *KCNQ1* gene expression in low-density cultured cardiomyocytes may indicate a decrease in I_{Ks} current in these cells. The decrease in KCNQ1 protein expression in Western blot analysis also supported this possibility, but there is uncertainty in the plasma membrane expression level of KCNQ1 channels. Since the increase in cell surface area is theoretically less than that of cell volume, the reduction of KCNQ1 protein level in whole cell lysate might not have caused the reduction of density of KCNQ1 channel in plasma membrane. This point remains to be clarified yet in future by using a membrane fraction. We suggest that the significant prolongation of FPD, ISI, and FPDc in low-density cells is due to changes in the expression of ion channels that contribute to action potential repolarization. However, the significant prolongation of basal FPDc in high-density (15,000 cells/probe) cultures is not likely a result of this same mechanism, because FPD and ISI were similar among high-, very high-, and middle-density (30,000 and 7500 cells/probe) cultures of cells. From a different viewpoint, the method used to correct FPD against ISI, Fridericia's formula ($FPDc = FPD/ISI^{1/3}$), may have caused this phenomenon. The action potential duration corresponding to FPD changes with alterations in the preceding interval of

excitation; therefore, FPD must be corrected by using some formula to compare the change on the basis of the same ISI. Because hiPSC-derived cardiomyocytes beat at around 60 bpm, we used Fridericia's formula, which typically is used for correction of the human QT interval (Funck-Brentano and Jaillon, 1993). However, this correction formula may not be optimal for hiPSC-derived cardiomyocytes and therefore may induce error into the correction. I_{Ks} current can contribute to the repolarization of cardiac action potentials but generally functions as a repolarization reserve. Therefore, in the basal state, inhibition of I_{Ks} current will not cause a notable change in action potential duration, but native cardiomyocytes activated through β-receptor stimulation demonstrate increased action potential duration by inhibition of I_{Ks} current (Volders et al., 2003). In hiPSC-derived cardiomyocytes, the prolongation of FPDc by I_{Ks} blockade by inhibitors suggests that the I_{Ks} current contributed to the repolarization of action potentials in cardiomyocytes at high density plating. Prolongation of FPDc by chromanol 293B and HMR1556 occurred at concentrations higher than 3 and 0.3 μM, respectively—higher than their respective reported IC_{50}s. The IC_{50} values of chromanol 293B and HMR1556 in *in vitro* voltage-clamp experiments in dog primary cardiomyocytes and artificial KCNQ1 and KCNE1-overexpressed cells have been reported to be 1.8–15.4 μM and 10.5–34 nM, respectively (Taniguchi et al., 2012; Thomas et al., 2003). The two following hypotheses may explain these differences in concentration. The first hypothesis is that the actual free concentrations of these agents in our experiments are lower than the nominal concentrations, because the assay medium for FPD measurement contained serum, and the binding of these compounds to proteins may have decreased the free concentration. The plasma protein binding ratio of HMR1556 is reported to be 75% (Nakashima et al., 2004), suggesting that the unbound concentrations of blockers might have been lower than the nominal concentration in the previous study (Taniguchi et al., 2012; Thomas et al., 2003). Because the main structure of chromanol 293B is the same as that of HMR1556 (Gogelein et al., 2000), putative protein-binding of chromanol 293B with a subsequent decrease in its free concentration is similarly possible. It may be possible to confirm this hypothesis if an appropriate serum-free medium becomes available. A second hypothesis for the differing concentrations of HMR1556 and

chromanol 293B between studies is that the contribution of I_{Kr} to FPD is far greater than that of I_{Ks} in the hiPSC-derived cardiomyocytes, so that increased concentrations of I_{Ks} blockers are needed to demonstrate effects. Moreover, our data on the effects of I_{Ks} and I_{Kr} channel blockers for FPDc measurement in hiPSC-derived cardiomyocytes corresponded to those from previous other reports using hiPSC- or hESC-derived cardiomyocytes treated with chromanol 293B (3–30 μM) or HMR1556 (1–3 μM) (Ma et al., 2011; Yamazaki et al., 2012). Therefore, we think that the decreased sensitivity of low-density cultured hiPSC-derived cardiomyocytes to FPDc prolongation after the application of I_{Ks} blockers can be interpreted as the presence of less I_{Ks} current compared with that in high-density cells. The induction of EAD by E4031 also supports the hypothesis that the I_{Ks} current was reduced by low-density plating because the similar observation was reported in cardiomyocytes obtained from dogs with chronic complete atrioventricular block (Volders et al., 1998).

Our analysis of ion channel expression revealed differences in gene expression between low- and high-density cell plating, as well as differences between hiPSC-derived cardiomyocytes and native human cardiac tissues. The difference between hiPSC-derived cardiomyocytes and human cardiac tissues may be caused by difference in the level of maturation, because hiPSC- and hESC-derived cardiomyocytes resemble fetal rather than adult cardiomyocytes in appearance, structure and function (Boheler et al., 2011; Ivashchenko et al., 2013). Another possible cause might be that the preparation of hiPSC-derived cardiomyocytes contains ventricular, atrial, nodal, and non-cardiac cells (Ma et al., 2011). Although the hiPSC-derived cardiomyocytes we used were purified to >97% cardiomyocytes by using selection methods based on the expression of cardiomyocyte-specific proteins and those with electrophysiological functions (Kattman et al., 2011), the resulting cultures nonetheless included various types of cardiac cells, and the maturation level of our cultured cardiomyocytes was unknown. The types and levels of ion channels active in cardiac cells change according to the developmental stage and differ between nodal, atrial, and ventricular cells. We consider that these factors influenced the observed differences between hiPSC-derived cardiomyocytes and primary human cardiac cells.

The I_{Ks} current is carried by potassium channels formed by oligomeric association of subunits coded by *KCNQ1* and *KCNE1* (Sanguinetti et al., 1996). Another KCNE subunit, *KCNE2*, also associates with *KCNQ1* subunit (Tinel et al., 2000). Mutations in *KCNQ1*, *KCNE1* and *KCNE2* can lead to QT prolongation and are responsible for long QT syndrome types 1, 5 and 6, respectively (Abbott et al., 1999; Keating & Sanguinetti, 2001; Priori et al., 1999; Wang et al., 1996). Inconsistent with the findings from the dog hypertrophy model (Ramakers et al. 2003), our study showed increased expression of *KCNE1*, the association subunit for I_{Ks} channels. Therefore, the contribution of the *KCNE1* subunit for I_{Ks} in cardiac hypertrophy remains to be clarified.

In previous studies of human adult hearts, *KCNE2* gene expression was much lower than that of the *KCNE1* gene, and *KCNQ1* gene expression was much higher than that of the KCNE subunits (Bendahhou et al., 2005; Lundquist et al., 2005). On this point, the difference of expression levels between *KCNQ1* and KCNE subunits were similar in our data, according to their threshold cycles (Ct) detected during qualitative PCR analysis (data not shown). Although the order of expression level is the same between hiPSC-derived cardiomyocytes and adult hearts, the interesting point is that expression of the *KCNE2* gene was higher in the hiPSC-derived cardiomyocytes than in human hearts. Co-expression of *KCNE2* with *KCNQ1* can lead to the formation of potassium channels but decreases current amplitude and abolishes the voltage- and time-dependence of channel activation compared with those observed for *KCNQ1* alone (Dedek & Waldegger, 2001; Tinel et al., 2000). However, owing to its high expression level, *KCNE2* may contribute to basal potassium current in hiPSC-derived cardiomyocytes. Decreases in I_{K1} current also have been reported in dog models (Volders et al., 1999), and the observed reduction in *KCNJ2* gene expression in low-density cultured hiPSC-derived cardiomyocytes is compatible with this earlier finding. However, we did not confirm the expression level of KCNJ2 protein because of its likely low concentration, according to its Ct value during qualitative PCR analysis (data not shown). Because the changes in the expression levels of the potassium channel genes involved in the repolarization of cardiac action potentials that we noted in low-density cultured hiPSC-derived cardiomyocytes occurred in the same direction as those in reported hypertrophy models, our model

likely will be useful in studying electrical remodeling during hypertrophic conditions.

Maturation of cardiomyocytes was not responsible for the observed alterations in gene expression, because the direction of changes in *KCNQ1*, *KCNJ2* and *KCNE1* were not mirrored in human fetal heart to adult heart. In addition, *ATP2A2* expression is increased in the developing heart (Chen et al., 2000; Gombosova et al., 1998; Piquereau et al., 2010), whereas *ATP2A2* expression was significantly lower in low-density cultured hiPSC-derived cardiomyocytes than in high-density cultured cells. Therefore, we conclude that the enlargement of hiPSC-derived cardiomyocytes represents a pathological hypertrophic phenomenon.

We suggest that hiPSC-derived cardiomyocytes—under low-density plating conditions only—can be used as a tool to elucidate the mechanisms underlying cardiac hypertrophy. hiPSC-derived cardiomyocytes are devoid of proliferating fibroblasts and can be cultured for several weeks, during which they retain spontaneous beating. Because of these advantages, hypertrophy-associated phenomena can be observed by using diverse electrophysiological, cell biological, and molecular biological methods in small hiPSC-derived cardiomyocytes from soon after plating until long after the cells become enlarged (that is, hypertrophic).

Figure Captions

Figure 1

Images of enlarged hiPSC-derived cardiomyocytes (CMs) and hypertrophic features of cells plated at various densities. hiPSC-derived cardiomyocytes were plated at 90,000 cells/well (high density, 2813 cells/mm^2) or 22,500 cells/well (low density, 703 cells/mm^2) on 96-well plates, incubated for 7 days. (A) Cells were stained with an anti-plasma–membrane stain (red) and imaged under a confocal fluorescent microscope with a 63× objective. Upper and right panels show cross-sectional cell heights at lines shown on the center panels. Long and short scale bars are 50 and 10 μm, respectively. (B) Cell areas were quantified. Horizontal bars in the plot show means ± SEM. Statistical significance was calculated by Welch's *t*-test. *** $P \leq 0.001$ (C) Cells were fixed with 4% paraformaldehyde, stained with anti-α-actinin antibody (green), an anti-cytoplasm and anti-nucleus stain (red), and an anti-nucleic acid stain (blue) and processed for fluorescence microscopy with a 20× objective. Scale bar is 50 μm. (D) hiPSC-derived cardiomyocytes were plated at 5.3×10^5 cells/well (high density, 2819 cells/mm^2) or 98,000 cells/well (low density, 521 cells/mm^2) in 24-well plates and incubated for 7 days. Cells were trypsinized and counted under a microscope before lysis. The protein concentration of each whole-cell lysate was determined by using the BCA protein assay, and the protein content per cell was calculated. Values are expressed as means ± SEM. Statistical significance was evaluated by using Welch's *t*-test. * $P \leq 0.05$.

Figure 2

Expression levels of genes associated with cardiac hypertrophy in hiPSC-derived cardiomyocytes (CMs), as determined by quantitative PCR. hiPSC-derived cardiomyocytes were plated at 2.7×10^6 cells/well (high density, 2813 cells/mm^2; $n = 3$) or 0.5×10^6 cells/well (low density, 521 cells/mm^2; $n = 3$) in 6-well plates and lysed to extract total RNA at 7 days after plating. Gene expressions were analyzed by using cDNA derived from total RNA isolated from cells. (A) Expression levels of housekeeping genes, *GAPDH*, *ACTB* and 18S rRNA in hiPSC-derived

cardiomyocytes and human fetal and adult heart tissue (B) Amounts of *NPPA*, *ATP2A2*, *ANKRD1*, and *MYL2* in hiPSC-derived cardiomyocytes were normalized relative to the expression level of 18S rRNA. Values are expressed as means ± SEM. Statistical significance was calculated by using Welch's *t*-test. * $P \leq 0.05$, ** $P \leq 0.01$, and *** $P \leq 0.001$.

Figure 3

Field-potential duration (FPD), inter-spike interval (ISI), and corrected FPD (FPDc) in hiPSC-derived cardiomyocytes plated at different densities. hiPSC-derived cardiomyocytes were plated at 30,000 cells/probe (very high density, 9554 cells/mm^2), 15,000 cells/probe (high density, 4777 cells/mm^2), 7500 cells/probe (medium density, 2389 cells/mm^2) or 3750 cells/probe (low density, 1194 cells/mm^2). FPD and ISI were measured by using the MED64 system. FPDc was calculated according to Fridericia's formula (FPDc = FPD/ISI$^{1/3}$). Values are expressed as means ± SEM. Statistical significance was calculated by Welch's *t*-test. * $P \leq 0.05$, ** $P \leq 0.01$, and *** $P \leq 0.001$ compared with values from very high density hiPSC-derived cardiomyocytes

Figure 4

Effects of I_{Ks} and I_{Kr} blockers on field potential duration (FPD) in hiPSC-derived cardiomyocytes plated at different densities. hiPSC-derived cardiomyocytes were plated at 30,000 cells/probe (very high density, 9554 cells/mm^2), 15,000 cells/probe (high density, 4777 cells/mm^2), 7500 cells/probe (medium density, 2389 cells/mm^2) or 3750 cells/probe (low density, 1194 cells/mm^2). FPD and inter-spike interval (ISI) were measured by using the MED64 system after the cells had been treated with the I_{Ks} blockers chromanol 293B (n = 1–8) or HMR1556 (n = 3–10) or with the I_{Kr} blocker E-4031 (n = 3–9). A corrected FPD (FPDc) was calculated according to Fridericia's formula (FPDc = FPD/ISI$^{1/3}$). (A) All FPDc were normalized to represent the percentage of change from the baseline value. Values are expressed as means ± SEM. Statistical significance was calculated by the Jonckheere-Terpstra trend test. * $P \leq 0.05$ and *** $P \leq 0.001$ evaluated cell-density-dependent effects, and Welch's *t*-test. # $P \leq 0.05$, and ## $P \leq 0.01$ compared with values from low density hiPSC-derived cardiomyocytes (3750 cells/probe) treated with E4031. (B) Typical

waveforms from low-density cells (3750 cells/probe) treated with DMSO as a baseline and those of early after depolarization (EAD) with 30 nM E4031 (arrows). EAD pattern was observed in 2 of 5 cases.

Figure 5

Expression levels of genes associated with I_{Ks} channel subunits and of potassium channel-related genes in hiPSC-derived cardiomyocytes (CMs) and human fetal and adult heart tissue. (A) Quantitative PCR; hiPSC-derived cardiomyocytes were plated at 2.7×10^6 cells/well (high density, 2813 cells/mm^2; $n = 3$) or 0.5×10^6 cells/well (low density, 521 cells/mm^2; $n = 3$) in 6-well plates and lysed to extract total RNA 7 days after plating. Amounts of *KCNQ1*, *KCNE1*, *KCNE2*, *KCNH2* and *KCNJ2* were analyzed by using cDNA derived from total RNA isolated from cells. All data were normalized relative to the expression level of 18S rRNA. Values are expressed as means ± SEM. Statistical significance was calculated by Welch's *t*-test. * $P \leq 0.05$, ** $P \leq 0.01$, *** $P \leq 0.001$, and **** $P \leq 0.0001$. (B) Western blotting. hiPSC-derived cardiomyocytes were plated at 5.3×10^5 cells/well (high density, 2819 cells/mm^2; $n = 4$) or 98,000 cells/well (low density, 521 cells/mm^2; $n = 3$) on 24-well plates and lysed to extract protein 7 days after plating. Samples of lysate corresponding to 10 μg of protein samples were denatured and used to detect KCNQ1 and KCNH2. The typical pictures of KCNQ1 and KCNH2 bands are shown. Molecular weight markers are indicated on the left. The arrows on the right show the 2 types of glycosylated KCNH2 proteins. (C) Quantification of KCNQ1 and KCNH2 proteins bands in Western blot. Values are expressed as means ± SEM. Statistical significance was calculated by Welch's *t*-test. * $P \leq 0.05$.

References

Abbott, G. W., Sesti, F., Splawski, I., Buck, M. E., Lehmann, M. H., Timothy, K. W., Keating, M. T., & Goldstein, S. A. (1999). MiRP1 forms IKr potassium channels with HERG and is associated with cardiac arrhythmia. *Cell, 97*, 175-187.

Aihara, Y., Kurabayashi, M., Saito, Y., Ohyama, Y., Tanaka, T., Takeda, S. i., Tomaru, K., Sekiguchi, K. i., Arai, M., Nakamura, T., & Nagai, R. (2000). Cardiac Ankyrin Repeat Protein Is a Novel Marker of Cardiac Hypertrophy : Role of M-CAT Element Within the Promoter. *Hypertension, 36*, 48-53.

Ancey, C., Menet, E., Corbi, P., Fredj, S., Garcia, M., Rucker-Martin, C., Bescond, J., Morel, F., Wijdenes, J., Lecron, J. C., & Potreau, D. (2003). Human cardiomyocyte hypertrophy induced in vitro by gp130 stimulation. *Cardiovascular Research, 59*, 78-85.

Anson, B. D., Kolaja, K. L., & Kamp, T. J. (2011). Opportunities for use of human iPS cells in predictive toxicology. *Clinical Pharmacology and Therapeutics, 89*, 754-758.

Bendahhou, S., Marionneau, C., Haurogne, K., Larroque, M. M., Derand, R., Szuts, V., Escande, D., Demolombe, S., & Barhanin, J. (2005). In vitro molecular interactions and distribution of KCNE family with KCNQ1 in the human heart. *Cardiovascular Research, 67*, 529-538.

Bernardo, B. C., Weeks, K. L., Pretorius, L., & McMullen, J. R. (2010). Molecular distinction between physiological and pathological cardiac hypertrophy: experimental findings and therapeutic strategies. *Pharmacology & Therapeutics, 128*, 191-227.

Boheler, K. R., Joodi, R. N., Qiao, H., Juhasz, O., Urick, A. L., Chuppa, S. L., Gundry, R. L., Wersto, R. P., & Zhou, R. (2011). Embryonic stem cell-derived cardiomyocyte heterogeneity and the isolation of immature and committed cells for cardiac remodeling and regeneration. *Stem Cells International, 2011*, 214203.

Chen, F., Ding, S., Lee, B. S., & Wetzel, G. T. (2000). Sarcoplasmic reticulum Ca(2+)ATPase and cell contraction in developing rabbit heart. *Journal of Molecular and Cellular Cardiology, 32*, 745-755.

Chen, H., Huang, X. N., Stewart, A. F., & Sepulveda, J. L. (2004). Gene expression changes associated with fibronectin-induced cardiac myocyte hypertrophy. *Physiological Genomics, 18*, 273-283.

Dedek, K., & Waldegger, S. (2001). Colocalization of KCNQ1/KCNE channel subunits in the mouse gastrointestinal tract. *Pflügers Archiv European Journal of Physiology, 442*, 896-902.

Drazner, M. H., Rame, J. E., Marino, E. K., Gottdiener, J. S., Kitzman, D. W., Gardin, J. M., Manolio, T. A., Dries, D. L., & Siscovick, D. S. (2004). Increased left ventricular mass is a risk factor for the development of a depressed left ventricular ejection fraction within five years: the Cardiovascular Health Study. *Journal of the American College of Cardiology, 43*, 2207-2215.

Egashira, T., Yuasa, S., Suzuki, T., Aizawa, Y., Yamakawa, H., Matsuhashi, T., Ohno, Y., Tohyama, S., Okata, S., Seki, T., Kuroda, Y., Yae, K., Hashimoto, H., Tanaka, T., Hattori, F., Sato, T., Miyoshi, S., Takatsuki, S., Murata, M., Kurokawa, J., Furukawa, T., Makita, N., Aiba, T., Shimizu, W., Horie, M., Kamiya, K., Kodama, I., Ogawa, S., & Fukuda, K. (2012). Disease characterization using LQTS-specific induced pluripotent stem cells. *Cardiovascular Research, 95*, 419-429.

Erokhina, I. L., Semenova, E. G., & Emel'ianova, O. I. (2005). Human fetal ventricular cardiomyocytes in vitro: proliferation and differentiation. *Tsitologiia, 47*, 200-206.

Flores-Munoz, M., Godinho, B. M., Almalik, A., & Nicklin, S. A. (2012). Adenoviral delivery of angiotensin-(1-7) or angiotensin-(1-9) inhibits cardiomyocyte hypertrophy via the mas or angiotensin type 2 receptor. *PloS One, 7*, e45564.

Foldes, G., Mioulane, M., Wright, J. S., Liu, A. Q., Novak, P., Merkely, B., Gorelik, J., Schneider, M. D., Ali, N. N., & Harding, S. E. (2011). Modulation of human embryonic stem cell-derived cardiomyocyte growth: a testbed for studying human cardiac hypertrophy? *Journal of Molecular and Cellular Cardiology, 50*, 367-376.

Frey, N., Katus, H. A., Olson, E. N., & Hill, J. A. (2004). Hypertrophy of the heart: a new

therapeutic target? *Circulation, 109*, 1580-1589.

Funck-Brentano, C., & Jaillon, P. (1993). Rate-corrected QT interval: techniques and limitations. *The American Journal of Cardiology, 72*, 17B-22B.

Gogelein, H., Bruggemann, A., Gerlach, U., Brendel, J., & Busch, A. E. (2000). Inhibition of IKs channels by HMR 1556. *Naunyn-Schmiedeberg's Archives of Pharmacology, 362*, 480-488.

Gombosova, I., Boknik, P., Kirchhefer, U., Knapp, J., Luss, H., Muller, F. U., Muller, T., Vahlensieck, U., Schmitz, W., Bodor, G. S., & Neumann, J. (1998). Postnatal changes in contractile time parameters, calcium regulatory proteins, and phosphatases. *The American Journal of Physiology, 274*, H2123-2132.

Hao, J., Kim, C. H., Ha, T. S., & Ahn, H. Y. (2007). Epigallocatechin-3 gallate prevents cardiac hypertrophy induced by pressure overload in rats. *Journal of Veterinary Science, 8*, 121-129.

Harmer, S. C., Wilson, A. J., Aldridge, R., & Tinker, A. (2010). Mechanisms of disease pathogenesis in long QT syndrome type 5. *American Journal of Physiology. Cell Physiology, 298*, C263-273.

Heineke, J., & Molkentin, J. D. (2006). Regulation of cardiac hypertrophy by intracellular signalling pathways. *Nature Reviews. Molecular Cell Biology, 7*, 589-600.

Ivashchenko, C. Y., Pipes, G. C., Lozinskaya, I. M., Lin, Z., Xiaoping, X., Needle, S., Grygielko, E. T., Hu, E., Toomey, J. R., Lepore, J. J., & Willette, R. N. (2013). Human-induced pluripotent stem cell-derived cardiomyocytes exhibit temporal changes in phenotype. *American Journal of Physiology. Heart and Circulatory Physiology, 305*, H913-922.

Jonckheere, A. R. (1954). A DISTRIBUTION-FREE k-SAMPLE TEST AGAINST ORDERED ALTERNATIVES. *Biometrika, 41*, 133-145.

Jost, N., Virag, L., Bitay, M., Takacs, J., Lengyel, C., Biliczki, P., Nagy, Z., Bogats, G., Lathrop, D. A., Papp, J. G., & Varro, A. (2005). Restricting excessive cardiac action potential and QT prolongation: a vital role for IKs in human ventricular muscle. *Circulation, 112*, 1392-1399.

Ju, H., Scammel-La Fleur, T., & Dixon, I. M. (1996). Altered mRNA abundance of calcium

transport genes in cardiac myocytes induced by angiotensin II. *Journal of Molecular and Cellular Cardiology, 28*, 1119-1128.

Kattman, S. J., Koonce, C. H., Swanson, B. J., & Anson, B. D. (2011). Stem cells and their derivatives: a renaissance in cardiovascular translational research. *Journal of Cardiovascular Translational Research, 4*, 66-72.

Keating, M. T., & Sanguinetti, M. C. (2001). Molecular and cellular mechanisms of cardiac arrhythmias. *Cell, 104*, 569-580.

Khan, J. M., Lyon, A. R., & Harding, S. E. (2013). The case for induced pluripotent stem cell-derived cardiomyocytes in pharmacological screening. *British Journal of Pharmacology, 169*, 304-317.

Li, G. R., Lau, C. P., Leung, T. K., & Nattel, S. (2004). Ionic current abnormalities associated with prolonged action potentials in cardiomyocytes from diseased human right ventricles. *Heart Rhythm : the Official Journal of the Heart Rhythm Society, 1*, 460-468.

Lundquist, A. L., Manderfield, L. J., Vanoye, C. G., Rogers, C. S., Donahue, B. S., Chang, P. A., Drinkwater, D. C., Murray, K. T., & George, A. L., Jr. (2005). Expression of multiple KCNE genes in human heart may enable variable modulation of I(Ks). *Journal of Molecular and Cellular Cardiology, 38*, 277-287.

Ma, J., Guo, L., Fiene, S. J., Anson, B. D., Thomson, J. A., Kamp, T. J., Kolaja, K. L., Swanson, B. J., & January, C. T. (2011). High purity human-induced pluripotent stem cell-derived cardiomyocytes: electrophysiological properties of action potentials and ionic currents. *American Journal of Physiology. Heart and Circulatory Physiology, 301*, H2006-2017.

Maron, B. J. (2002). Hypertrophic cardiomyopathy: a systematic review. *JAMA : the Journal of the American Medical Association, 287*, 1308-1320.

Maron, M. S., Olivotto, I., Betocchi, S., Casey, S. A., Lesser, J. R., Losi, M. A., Cecchi, F., & Maron, B. J. (2003). Effect of left ventricular outflow tract obstruction on clinical outcome in hypertrophic cardiomyopathy. *The New England Journal of Medicine, 348*, 295-303.

Melman, Y. F., Krummerman, A., & McDonald, T. V. (2002). KCNE regulation of KvLQT1

channels: structure-function correlates. *Trends in Cardiovascular Medicine, 12*, 182-187.

Nakashima, H., Gerlach, U., Schmidt, D., & Nattel, S. (2004). In vivo electrophysiological effects of a selective slow delayed-rectifier potassium channel blocker in anesthetized dogs: potential insights into class III actions. *Cardiovascular Research, 61*, 705-714.

Ogawa, E., Saito, Y., Harada, M., Kamitani, S., Kuwahara, K., Miyamoto, Y., Ishikawa, M., Hamanaka, I., Kajiyama, N., Takahashi, N., Nakagawa, O., Masuda, I., Kishimoto, I., & Nakao, K. (2000). Outside-in signalling of fibronectin stimulates cardiomyocyte hypertrophy in cultured neonatal rat ventricular myocytes. *Journal of Molecular and Cellular Cardiology, 32*, 765-776.

Piquereau, J., Novotova, M., Fortin, D., Garnier, A., Ventura-Clapier, R., Veksler, V., & Joubert, F. (2010). Postnatal development of mouse heart: formation of energetic microdomains. *The Journal of Physiology, 588*, 2443-2454.

Priori, S. G., Barhanin, J., Hauer, R. N., Haverkamp, W., Jongsma, H. J., Kleber, A. G., McKenna, W. J., Roden, D. M., Rudy, Y., Schwartz, K., Schwartz, P. J., Towbin, J. A., & Wilde, A. (1999). Genetic and molecular basis of cardiac arrhythmias; impact on clinical management. Study group on molecular basis of arrhythmias of the working group on arrhythmias of the european society of cardiology. *European Heart Journal, 20*, 174-195.

Ramakers, C., Vos, M. A., Doevendans, P. A., Schoenmakers, M., Wu, Y. S., Scicchitano, S., Iodice, A., Thomas, G. P., Antzelevitch, C., & Dumaine, R. (2003). Coordinated down-regulation of KCNQ1 and KCNE1 expression contributes to reduction of I(Ks) in canine hypertrophied hearts. *Cardiovascular Research, 57*, 486-496.

Roden, D. M., Lazzara, R., Rosen, M., Schwartz, P. J., Towbin, J., & Vincent, G. M. (1996). Multiple mechanisms in the long-QT syndrome. Current knowledge, gaps, and future directions. The SADS Foundation Task Force on LQTS. *Circulation, 94*, 1996-2012.

Sadoshima, J., Xu, Y., Slayter, H. S., & Izumo, S. (1993). Autocrine release of angiotensin II mediates stretch-induced hypertrophy of cardiac myocytes in vitro. *Cell, 75*, 977-984.

Sanguinetti, M. C., Curran, M. E., Zou, A., Shen, J., Spector, P. S., Atkinson, D. L., & Keating, M.

T. (1996). Coassembly of K(V)LQT1 and minK (IsK) proteins to form cardiac I(Ks) potassium channel. *Nature, 384*, 80-83.

Schroeder, A., Mueller, O., Stocker, S., Salowsky, R., Leiber, M., Gassmann, M., Lightfoot, S., Menzel, W., Granzow, M., & Ragg, T. (2006). The RIN: an RNA integrity number for assigning integrity values to RNA measurements. *BMC Molecular Biology, 7*, 3.

Shubeita, H. E., McDonough, P. M., Harris, A. N., Knowlton, K. U., Glembotski, C. C., Brown, J. H., & Chien, K. R. (1990). Endothelin induction of inositol phospholipid hydrolysis, sarcomere assembly, and cardiac gene expression in ventricular myocytes. A paracrine mechanism for myocardial cell hypertrophy. *The Journal of Biological Chemistry, 265*, 20555-20562.

Stengl, M., Ramakers, C., Donker, D. W., Nabar, A., Rybin, A. V., Spatjens, R. L., van der Nagel, T., Wodzig, W. K., Sipido, K. R., Antoons, G., Moorman, A. F., Vos, M. A., & Volders, P. G. (2006). Temporal patterns of electrical remodeling in canine ventricular hypertrophy: focus on IKs downregulation and blunted beta-adrenergic activation. *Cardiovascular Research, 72*, 90-100.

Taniguchi, T., Uesugi, M., Arai, T., Yoshinaga, T., Miyamoto, N., & Sawada, K. (2012). Chronic probucol treatment decreases the slow component of the delayed-rectifier potassium current in CHO cells transfected with KCNQ1 and KCNE1: a novel mechanism of QT prolongation. *Journal of Cardiovascular Pharmacology, 59*, 377-386.

Terpstra, T. J. (1952). The asymptotic normality and consistency of Kendall's test against trend, when ties are present in one ranking. *Indigationes Mathematicae, 14*, 327-333.

Thomas, G. P., Gerlach, U., & Antzelevitch, C. (2003). HMR 1556, a potent and selective blocker of slowly activating delayed rectifier potassium current. *Journal of Cardiovascular Pharmacology, 41*, 140-147.

Tinel, N., Diochot, S., Borsotto, M., Lazdunski, M., & Barhanin, J. (2000). KCNE2 confers background current characteristics to the cardiac KCNQ1 potassium channel. *The EMBO Journal, 19*, 6326-6330.

Tulloch, N. L., Muskheli, V., Razumova, M. V., Korte, F. S., Regnier, M., Hauch, K. D., Pabon, L., Reinecke, H., & Murry, C. E. (2011). Growth of engineered human myocardium with mechanical loading and vascular coculture. *Circulation Research, 109*, 47-59.

Vakili, B. A., Okin, P. M., & Devereux, R. B. (2001). Prognostic implications of left ventricular hypertrophy. *American Heart Journal, 141*, 334-341.

Volders, P. G., Sipido, K. R., Vos, M. A., Spatjens, R. L., Leunissen, J. D., Carmeliet, E., & Wellens, H. J. (1999). Downregulation of delayed rectifier K(+) currents in dogs with chronic complete atrioventricular block and acquired torsades de pointes. *Circulation, 100*, 2455-2461.

Volders, P. G., Stengl, M., van Opstal, J. M., Gerlach, U., Spatjens, R. L., Beekman, J. D., Sipido, K. R., & Vos, M. A. (2003). Probing the contribution of IKs to canine ventricular repolarization: key role for beta-adrenergic receptor stimulation. *Circulation, 107*, 2753-2760.

Volders, P. G. A., Sipido, K. R., Vos, M. A., Kulcsar, A., Verduyn, S. C., & Wellens, H. J. J. (1998). Cellular Basis of Biventricular Hypertrophy and Arrhythmogenesis in Dogs With Chronic Complete Atrioventricular Block and Acquired Torsade de Pointes. *Circulation, 98*, 1136-1147.

Wang, Q., Curran, M. E., Splawski, I., Burn, T. C., Millholland, J. M., VanRaay, T. J., Shen, J., Timothy, K. W., Vincent, G. M., de Jager, T., Schwartz, P. J., Toubin, J. A., Moss, A. J., Atkinson, D. L., Landes, G. M., Connors, T. D., & Keating, M. T. (1996). Positional cloning of a novel potassium channel gene: KVLQT1 mutations cause cardiac arrhythmias. *Nature Genetics, 12*, 17-23.

Watkins, S. J., Borthwick, G. M., & Arthur, H. M. (2011). The H9C2 cell line and primary neonatal cardiomyocyte cells show similar hypertrophic responses in vitro. *In Vitro Cellular & Developmental Biology. Animal, 47*, 125-131.

Yamazaki, K., Hihara, T., Taniguchi, T., Kohmura, N., Yoshinaga, T., Ito, M., & Sawada, K. (2012). A novel method of selecting human embryonic stem cell-derived cardiomyocyte clusters for

assessment of potential to influence QT interval. *Toxicology in Vitro : An International Journal Published in Association with BIBRA, 26*, 335-342.

Zou, M. X., Roy, A. A., Zhao, Q., Kirshenbaum, L. A., Karmazyn, M., & Chidiac, P. (2006). RGS2 is upregulated by and attenuates the hypertrophic effect of alpha1-adrenergic activation in cultured ventricular myocytes. *Cellular Signalling, 18*, 1655-1663.

Figure 1

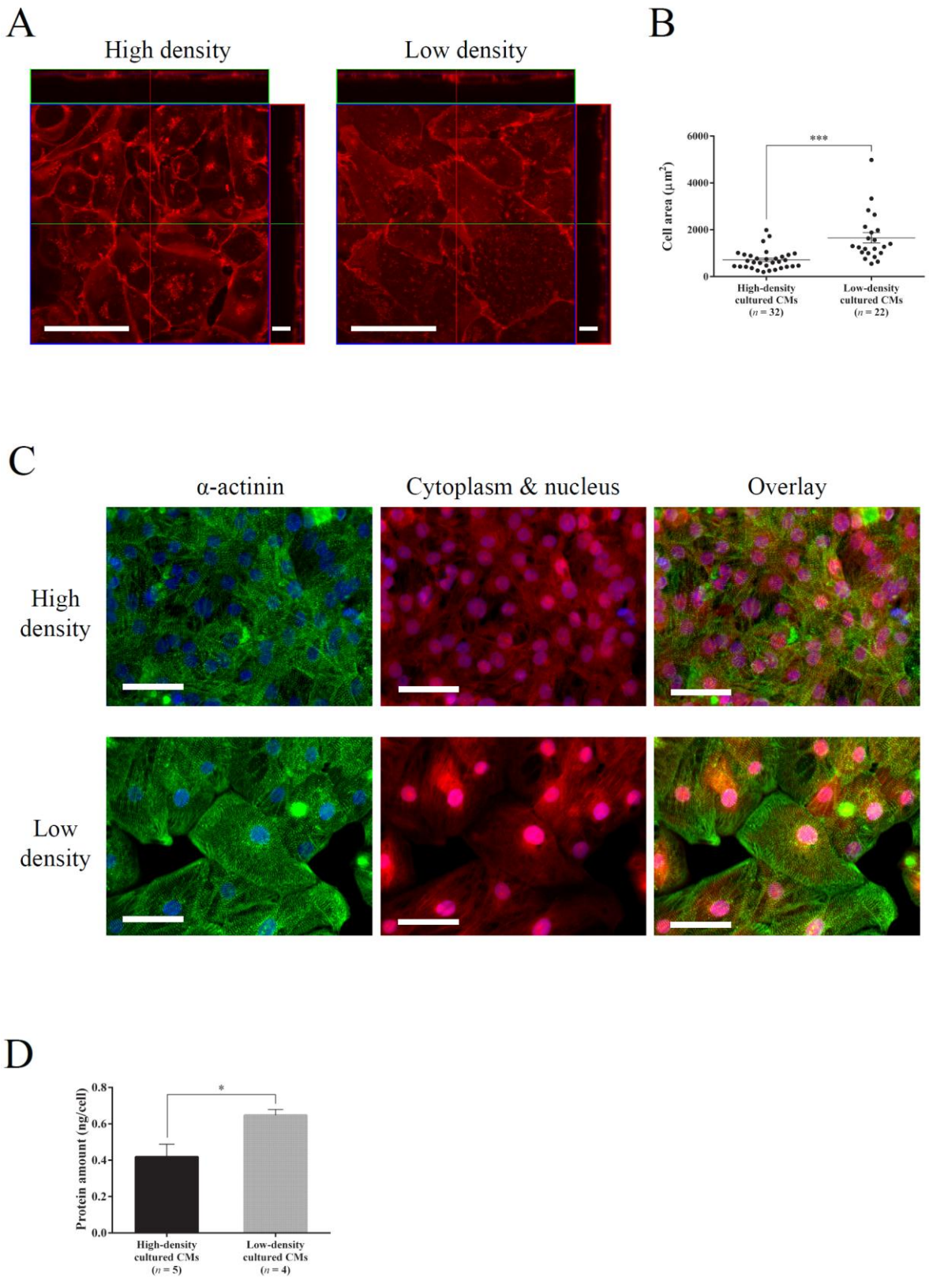
A
High density
Low density
B
Cell area (μm²)
6000
4000
2000
0
***
High-density cultured CMs (n = 32)
Low-density cultured CMs (n = 22)
C
α-actinin
Cytoplasm & nucleus
Overlay
High density
Low density
D
Protein amount (ng/cell)
0.8
0.6
0.4
0.2
0.0
*
High-density cultured CMs (n = 5)
Low-density cultured CMs (n = 4)

Table 1
Pathway analysis using DNA microarray data from low-density cultured hiPSC-derived cardiomyocytes to show overlaps in functional gene lists.

Category	Function annotation	*P*
Cardiac Hypertrophy	**hypertrophy of heart chamber**	**0.000004**
Cardiac Hypertrophy	**hypertrophy of heart**	**0.000006**
Cardiac Hypertrophy	**hypertrophy of left ventricle**	**0.000007**
Cardiac Hypertrophy	**ventricular hypertrophy**	**0.000009**
Cardiac Arteriopathy	coronary artery disease	0.000010
Liver Hyperplasia/Hyperproliferation	liver cancer and tumors	0.000025
Liver Hyperplasia/Hyperproliferation	liver cancer	0.000028
Cardiac Necrosis/Cell Death	cell death of heart	0.000038
Cardiac Dilation	dilation of heart ventricle	0.000237
Cardiac Dilation	dilation of heart chamber	0.000295

Listed are the top 10 of Tox Functions provided by using Ingenuity Pathway Analysis related to the list[a] of gene probes in low-density cultured hiPSC-derived cardiomyocytes with a fold change of ≥ 1.5 and a false discovery rate *P*-value of ≤ 0.05 compared with high-density cultured cells. Bold text indicates cardiac-hypertrophy–related pathway. *P*: *P*-value calculated by Fisher's exact test.

[a] hiPSC-derived cardiomyocytes were plated at a density of 2.7×10^6 cells/well (high density, 2813 cells/mm^2; n = 3) or 0.5×10^6 cells/well (low density, 521 cells/mm^2; n = 3) in 6-well plates, incubated for 7 days, and lysed to extract total RNA. All gene expression data were normalized by using the quantile method. Expression changes are shown as fold changes compared with values in high-density cultured hiPSC-derived cardiomyocytes. Statistical significance was calculated by using Welch's *t*-test, followed by adjustment for multiple comparisons by using a false discovery rate approach (Benjamini–Hochberg procedure).

Figure 2

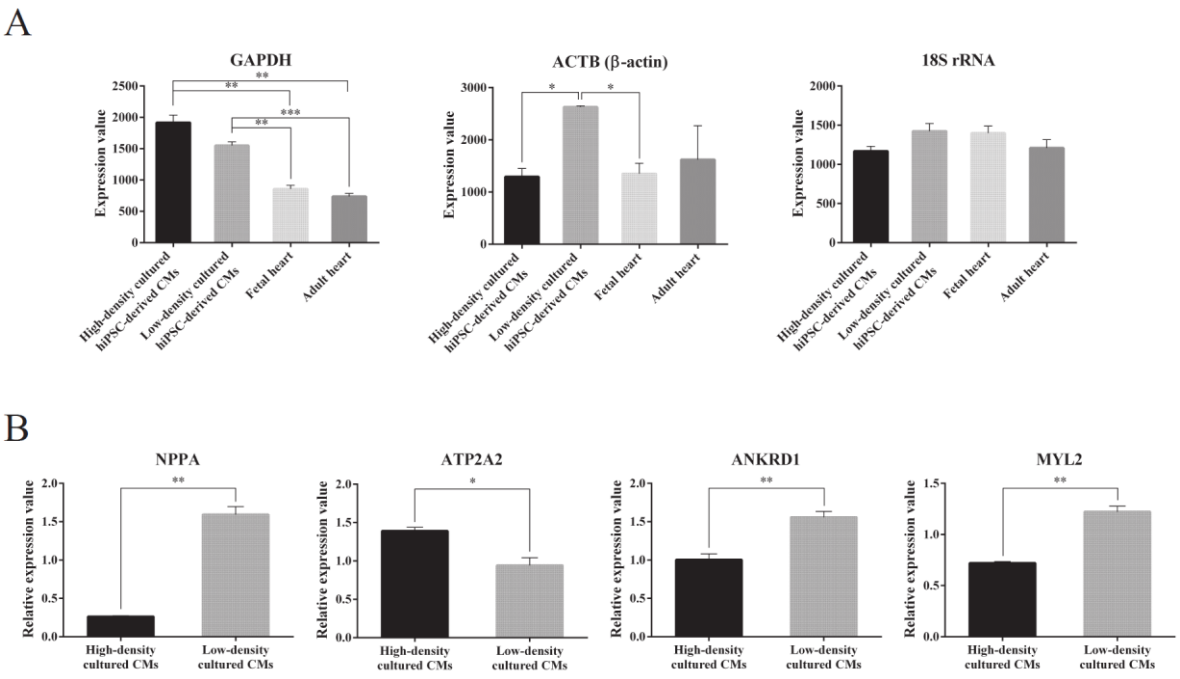
A
GAPDH
ACTB (β-actin)
18S rRNA
Expression value
High-density cultured hiPSC-derived CMs
Low-density cultured hiPSC-derived CMs
Fetal heart
Adult heart
B
NPPA
ATP2A2
ANKRD1
MYL2
Relative expression value
High-density cultured CMs
Low-density cultured CMs

Figure 3

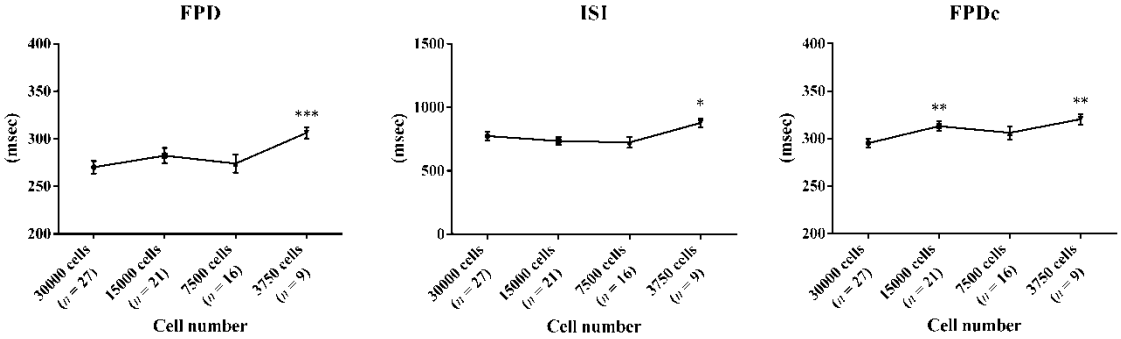
FPD
ISI
FPDc
(msec)
400
350
300
250
200
1500
1000
500
0
***
*
**
**
30000 cells (n = 27)
15000 cells (n = 21)
7500 cells (n = 16)
3750 cells (n = 9)
Cell number

Figure 4

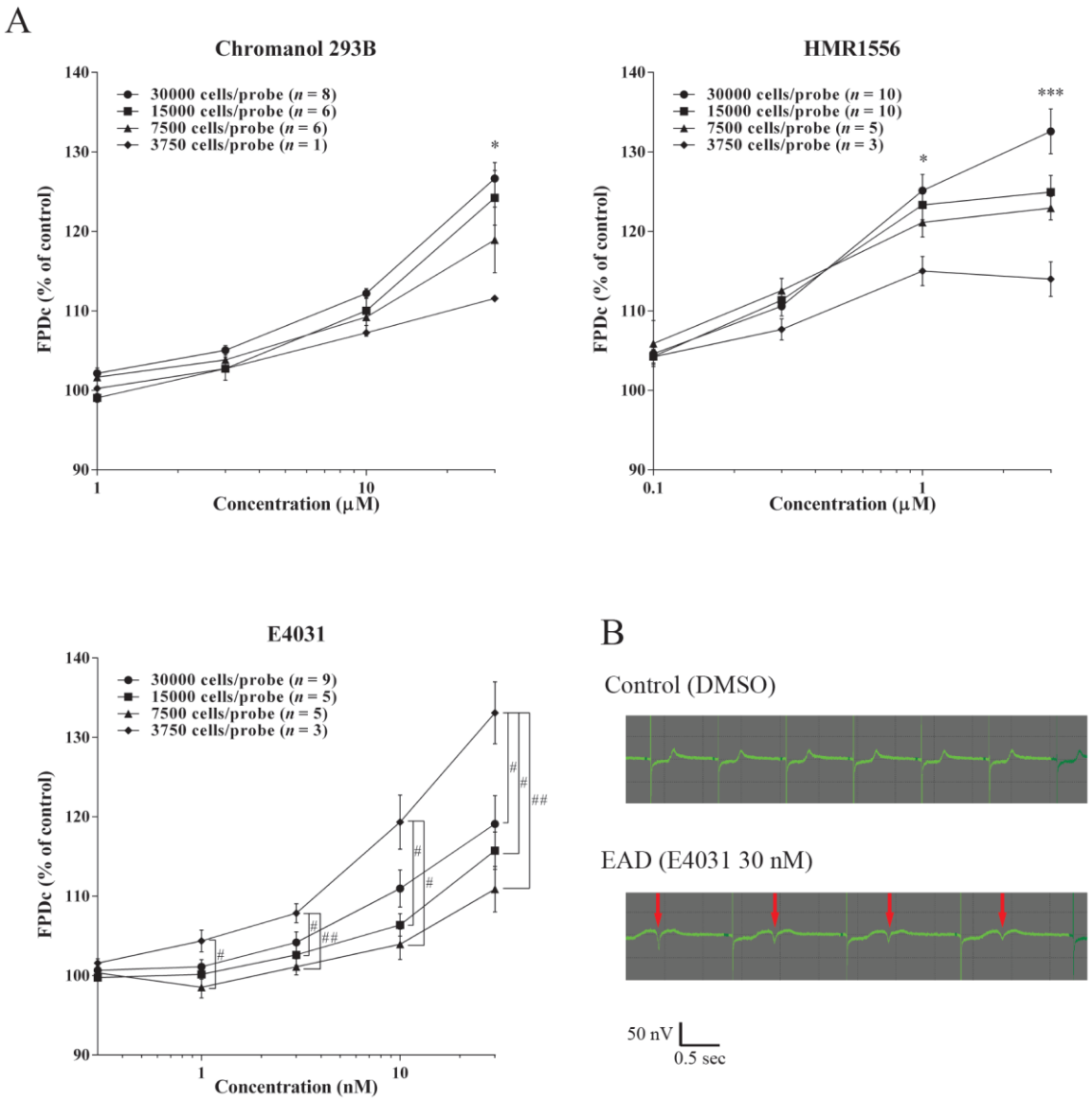
A
Chromanol 293B
30000 cells/probe (n = 8)
15000 cells/probe (n = 6)
7500 cells/probe (n = 6)
3750 cells/probe (n = 1)
FPDc (% of control)
Concentration (μM)
HMR1556
30000 cells/probe (n = 10)
15000 cells/probe (n = 10)
7500 cells/probe (n = 5)
3750 cells/probe (n = 3)
FPDc (% of control)
Concentration (μM)
E4031
30000 cells/probe (n = 9)
15000 cells/probe (n = 5)
7500 cells/probe (n = 5)
3750 cells/probe (n = 3)
FPDc (% of control)
Concentration (nM)
B
Control (DMSO)
EAD (E4031 30 nM)
50 nV
0.5 sec

Figure 5

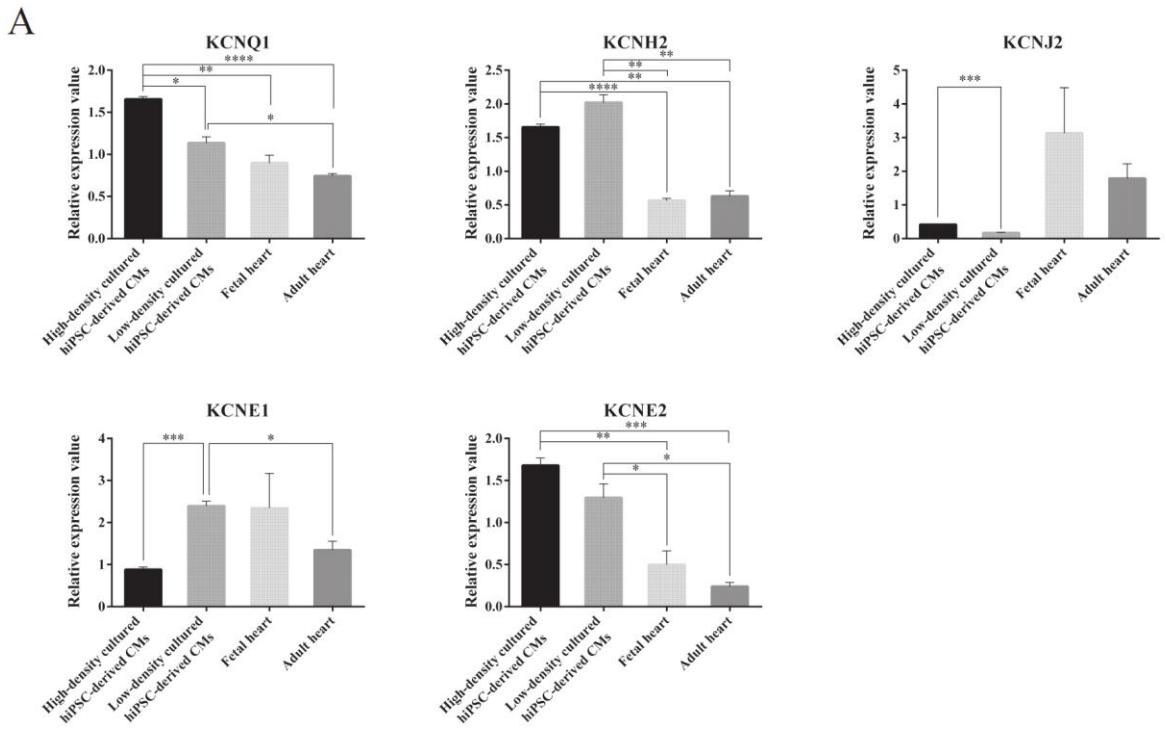
A
KCNQ1
KCNH2
KCNJ2
KCNE1
KCNE2
Relative expression value
High-density cultured hiPSC-derived CMs
Low-density cultured hiPSC-derived CMs
Fetal heart
Adult heart
B
High density
Low density
70 kD
KCNQ1
130 kD
KCNH2
C
KCNQ1
KCNH2
Intensity
High-density cultured CMs (n = 4)
Low-density cultured CMs (n = 3)

参　考　論　文

Uesugi, M., Ojima, A., Taniguchi, T., Miyamoto, N., & Sawada, K. (2013). Low-density plating is sufficient to induce cardiac hypertrophy and electrical remodeling in highly purified human iPS cell-derived cardiomyocytes. *Journal of Pharmacological and Toxicological Methods*. (DOI#10.1016/j.vascn.2013.11.002)